Calix[*n*]bispyrrolylbenzenes: Synthesis, Characterization, and Preliminary Anion Binding Studies

Jonathan L. Sessler,*[a] Deqiang An,[a] Won-Seob Cho,[a] Vincent Lynch,[a] and Manuel Marquez[b]

Abstract: A series of novel calixpyrrole-like macrocycles, calix[*n*]bis(pyrrol-2-yl)benzene (calix[*n*]BPBs, $n=2$–4) **9a**–**11a**, have been synthesized by means of the TFA-catalyzed condensation reaction of bis(pyrrol-2-yl)benzene **8a** with acetone. Calix[2]BPB **9a** represents an expanded version of calix[4]pyrrole in which two of the four *meso* bridges are replaced by benzene rings. By contrast, systems **10a** and **11a**, which bear great considerable to calixbipyrroles **2** and **3**, represent higher homologues of the basic calix[*n*]BPB motif. Solution-phase anion binding studies, carried out by means of ^{1}H NMR spectroscopic titrations in [D_2]dichloromethane and isothermal titration calorimetry (ITC) in 1,2-dichloroethane, reveal that **9a** binds typical small anions with substantially higher affinities than **1**, even though the same number of hydrogen bonding donor groups are found in both compounds. The basic building block for **9a**, benzene dipyrrole **8a**, also displays a higher affinity for anions than the building block for **1**, dimethyldipyrromethane **16**. Structural studies, carried out by single-crystal X-ray diffraction analyses, are consistent with the solution-phase results and reveal that **9a** is able to stabilize complexes with chloride and nitrate in the solid state. Structures of the PF_6^- and NO_3^- complexes of **10a** were also solved as were those of the acetone adduct of **9a** and the ethyl acetate adduct of **11a**.

Keywords: anions · hydrogen bonds · macrocycles · molecular recognition · receptors

Introduction

In recent years, considerable effort has been focused on the generalized problem of anion recognition. This has led, among other things, to the design and synthesis of a number of highly sophisticated receptor systems, including ones that display very specific anion-binding selectivities. It has also spawned efforts to produce simpler systems whose ease of synthesis might serve to overcome any lack of inherent design specificity and which might offer advantages, on a pure cost of good basis, when used in various "real world" applications.[1–6] Among the more attractive of the easy-to-prepare anion-binding systems is calix[4]pyrrole.[1] Assembled in one high-yielding step from commercially available starting materials, calix[4]pyrroles (e.g., **1**) have been found to bind small anions, such as fluoride and chloride, with good affinity in aprotic solvents. Such findings, in turn, have inspired efforts aimed at extending the chemistry of calix[4]-pyrroles. To date, this has been done through the preparation of larger calix[*n*]pyrrole systems ($n>4$)[7–10] and through the formal replacement of one or more of the pyrrole rings by some other aromatic subunit, for example, pyridine,[11] benzene,[12] furan, or thiophene.[13] We have also recently found that bipyrrole may be used as a "building block" and

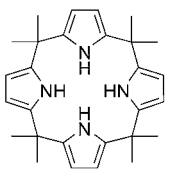

1

[a] Prof. J. L. Sessler, D. An, W.-S. Cho, V. Lynch
Department of Chemistry and Biochemistry
Institute of Cellular and Molecular Biology
The University of Texas at Austin
1 University Station-A5300, Austin, TX 78712-1167 (USA)
Fax: (+1) 512-471-7550
E-mail: sessler@mail.utexas.edu

[b] Dr. M. Marquez
Chemical Science and Technology Division
Los Alamos National Laboratory
Los Alamos, NM 87545 (USA)
and
I'NEST Group, New Technology Research Department, PMUSA
Richmond, VA 23298 (USA)

Supporting information for this article is available on the WWW under http://www.chemeurj.org/ or from the author.

 DOI: 10.1002/chem.200400894

have reported the synthesis of calix[*n*]bipyrroles **2** and **3** ($n=3$, 4)[14] and calix[2]bipyrrole[2]furan and calix[2]bipyrrole[2]thiophene systems (e.g., **4** and **5**).[15] In independent

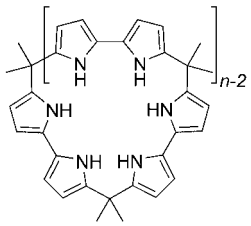

2: $n=3$
3: $n=4$

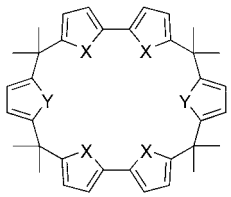

4: X = NH; Y = O
5: X = NH; Y = S
6: X = S; Y = NH

work, Lee's group has also reported the synthesis of a macrocycle, **6**, that is based on pyrrole and bithiophene.[16] The finding that systems **2**, **4**, and **5**, in particular, act as highly effective anion-binding agents[14,15] led us to consider the next logical step, namely the use of terpyrrole (**7**) as the key pyrrole-containing building block. Unfortunately, to date we have been unable to isolate any stable products from condensation reactions involving terpyrrole **7** and various ketones (e.g., acetone). However, we have now found that an alternative precursor, namely 1,3-bis(pyrrol-2-yl)benzene (BPB, **8**), shows considerable promise as a building block and wish to report here the synthesis and characterization of the calix[*n*]1,3-bis(pyrrol-2-yl)benzenes **9**–**11**; these large cyclophane-like systems differ in terms of the size of the calix core ($n=2$, 3, and 4) and the nature of 5-substituent on the benzene rings (series **a**, **b**, and **c**). We also wish to report the results of preliminary anion binding studies carried out with **8a**–**11a**. One of these receptors, system **9a**, in spite of containing the same number of pyrrole NH hydrogen-bond donor groups (four), displays an affinity for many anions, including perchlorate, that is enhanced relative to that of calix[4]pyrrole **1**.

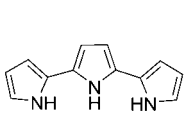

7

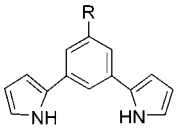

8a-c

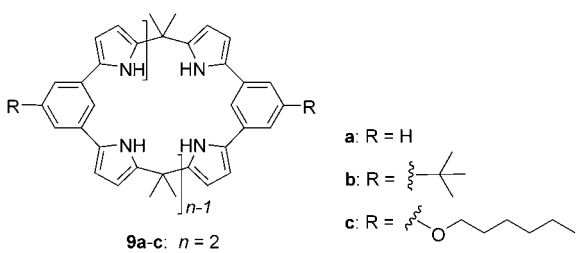

9a-c: $n=2$
10a-c: $n=3$
11a-c: $n=4$

a: R = H
b: R =
c: R =

Results and Discussion

Synthesis and crystal structures: The synthesis of target molecules **9**–**11** is shown in Scheme 1. Here, the key 1,3-bis(pyrrol-2-yl)benzene precursors, **8a**–**c**, were synthesized by using a modification of a literature method used to prepare 1,4-bis(pyrrol-2-yl)benzene.[17] Intermediates **12a**,**b** were then obtained from the reaction of the corresponding isophthaloyl chlorides, **13** and **14**, with allylamine and triethylamine in dichloromethane. The ether-functionalized system **12c** was obtained by the aminolysis of dimethyl-5-hexyloxyisophthalate **15** in the presence of allylamine. Reaction of **12a**–**c** with phosgene (to give the presumed imino chloride derivatives), followed by immediate reaction with potassium *tert*-butoxide in THF afforded **8a**–**c** in yields of 29%, 43%, and 96%, respectively. The electron-donating groups at the 5-position of the benzene rings are expected to stabilize the intermediate carbocations formed during the reaction, thus accounting for the increased yields observed on passing from **8a** to **8c**. Stirring intermediates **8a**–**c** in acetone overnight in the presence of one equivalent of trifluoroacetic acid afforded products **9a**–**c**, **10a**–**c**, and **11a**–**c**. All new compounds were characterized by standard spectroscopic techniques, including ^{1}H and ^{13}C NMR spectroscopy, and high-resolution mass spectrometry (HRMS). Compounds **9a**, **10a**, **11a**, and **8a** were also characterized by X-ray diffraction analysis.

An X-ray structural analysis of **8a** revealed that the molecule adopts a "*cis*-" conformation in solid state and contains an internal symmetry plane. Both pyrrole NH donor groups point in towards the center of the resulting cleft (Figure 1 top), but are twisted out of the plane defined by the benzene ring with N1-C4-C5-C6 torsion angles of 23.48° (c.f., Figure 1 middle). No evidence of π stacking is observed in the packing diagram. However, the possibility of intermolecular hydrogen-bonding interactions of the NH–π type involving the pyrrole-NH protons of one molecule and the benzene π-electrons of another can be inferred from this same packing profile (Figure 1 bottom).

Diffraction grade crystals of **9a**·2$(CH_3)_2CO$ were obtained by slow evaporation of a solution of **9a** in dichloromethane and acetone. X-ray analysis revealed that the molecule adopts a 1,2-alternate (C_{2h}) conformation (Figure 2). The two benzene rings, although on opposite sides of the molecule, are nearly coplanar. By contrast, the pyrrolic subunits connected to each of the two *meso*-carbon atoms are tilted out of the plane defined by the benzene rings. Each of the two pyrrole units around the bridging *meso*-carbon atoms is hydrogen bonded (NH···O) to one acetone molecule and each pair points to a different side of the plane. The N–O distances are in the range of 3.033(3)–3.122(3) Å, the NH H–O distances are in the range of 2.12(3)–2.16(3) Å, and the N-H-O angles are in the range of 167(2)–177(3)°. The X-ray analysis also revealed that the host molecule uses the two sets of pyrrole units bound to the two *meso*-carbon atoms, or more precisely, their NH donor subunits, to interact with the bound acetone molecules, rather than the alter-

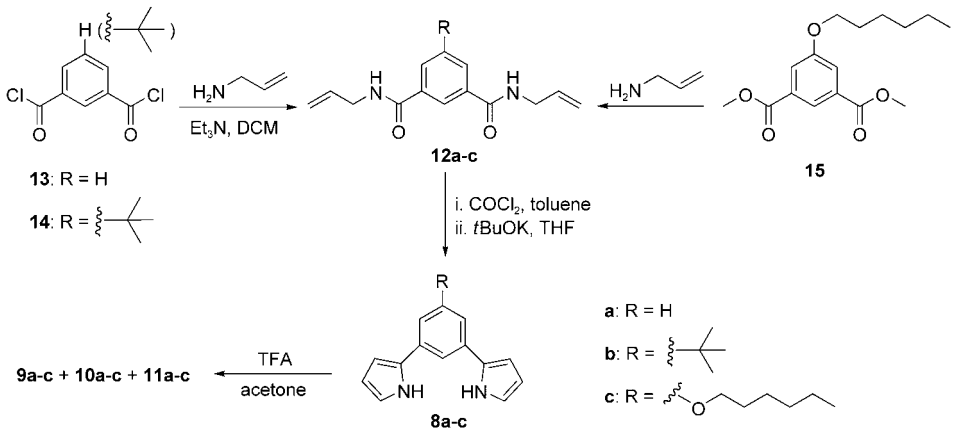

Scheme 1. Synthesis of **9a–c**, **10a–c**, and **11a–c**.

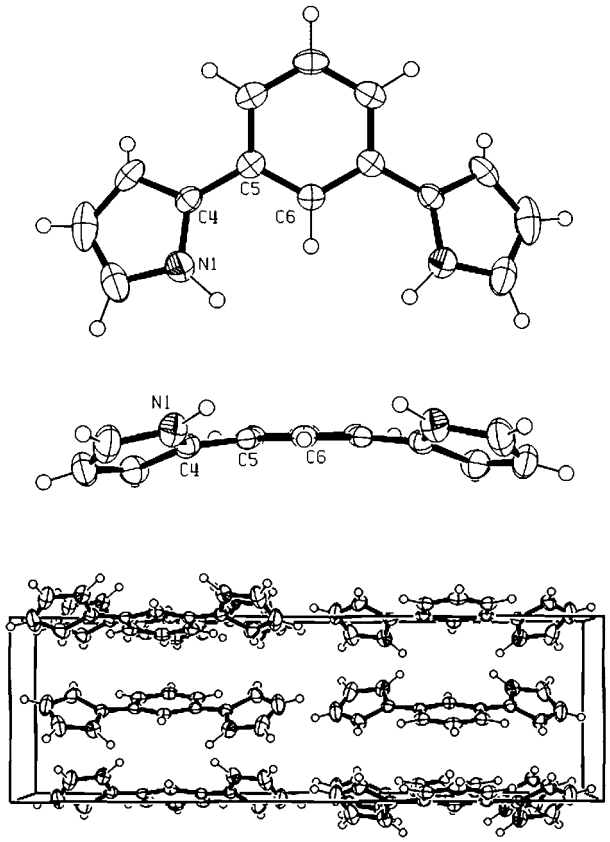

Figure 1. X-ray crystal structure of **8a** (ORTEP, displacement ellipsoids scaled to the 50% probability level). Top: top view; middle: side view; bottom: unit-cell packing diagram.

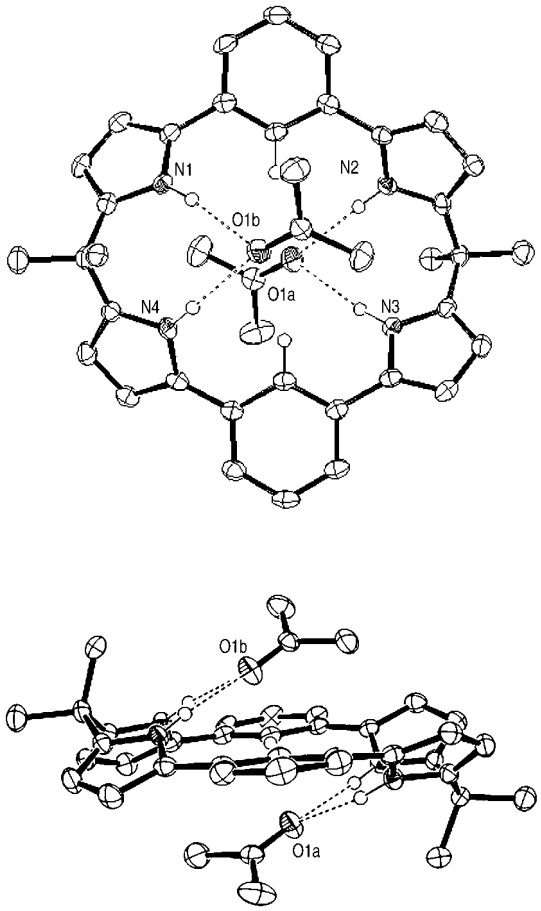

Figure 2. X-ray crystal structure of **9a**·2$(CH_3)_2CO$ (ORTEP, displacement ellipsoids scaled to the 50% probability level; some hydrogen atoms have been removed for clarity). Top: top view; bottom: side view. Dashed lines are indicative of N–H···O hydrogen bonds.

native pairing of the pyrrole subunits attached to the two benzene rings.

The hydrogen-bonding interactions seen between macrocycle **9a** and acetone in the solid state led to the consideration that **9a** might also act as a receptor for anions of appropriate size and shape. Preliminary support for this notion came from a single-crystal X-ray structural analysis of the chloride anion complex of **9a** (tetrabutylammonium, TBA, counterion); it revealed that **9a** adopts a cone-shaped (or V-shaped, C_{2v}) conformation in the solid state, with four pyrrole NH protons involved in hydrogen-bonding interactions to the chloride anion (Figure 3). The N–Cl distances are in the range of 3.306(3)–3.401(3) Å, while the corresponding NH H–Cl distances range between 2.37(3) and 2.58(2) Å. The chloride ion resides 1.377(4) Å above the N_4 root-mean-square plane of the core of **9a**. The N-H-Cl angles are in the range of 169–177°. The distances between the CH protons (2-position of BPB benzene ring) and the bound chloride anion are 2.588 Å and 2.721 Å, respectively, while the corresponding C-H-Cl angles are 157.88 and 162.60°. These parameters are within the range expected for hydro-

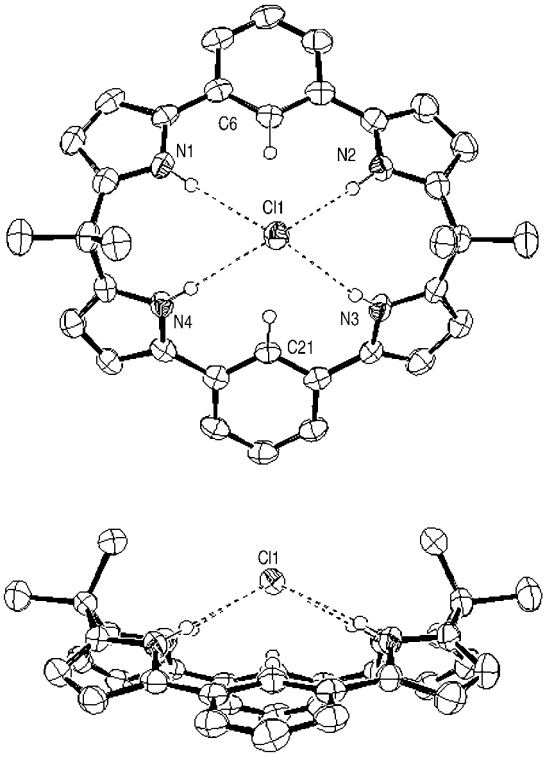

Figure 3. X-ray crystal structure of **9a**·Cl^- (ORTEP, displacement ellipsoids scaled to the 50% probability level; some hydrogen atoms have been removed for clarity). Top: top view; bottom: side view. Dashed lines are indicative of N–H···Cl^- hydrogen bonds.

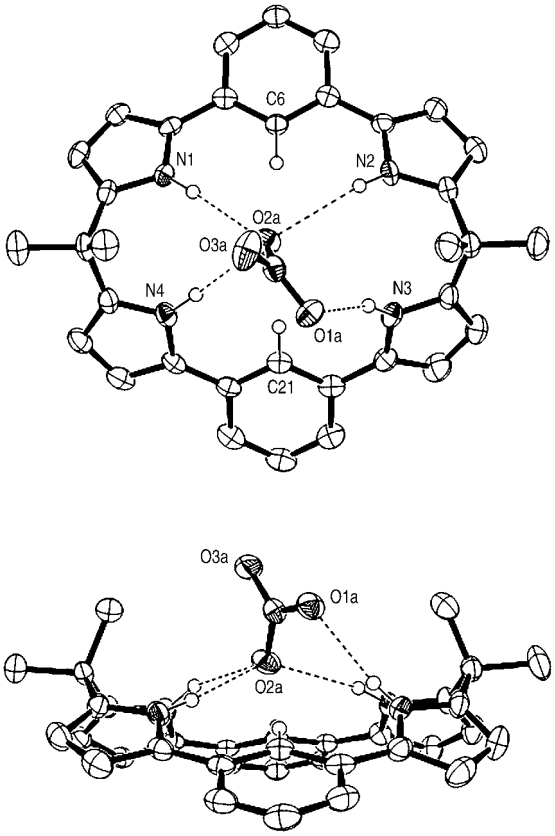

Figure 4. X-ray crystal structure of **9a**·NO_3^- (ORTEP, displacement ellipsoids scaled to the 50% probability level; some hydrogen atoms have been removed for clarity). Top: top view; bottom: side view. Dashed lines are indicative of N–H···O hydrogen bonds.

gen-bonding interactions, leading to the consideration that these CH protons may also be acting to stabilize the bound chloride anion.

Diffraction-grade crystals of **9a**·NO_3^- were also obtained by using conditions analogous to those used to obtain crystals of **9a**·Cl^-. X-ray structural analysis shows that, as is true for **9a**·Cl^-, the macrocycle adopts a cone-like conformation in the solid state and interacts with the bound nitrate anion through four NH···O hydrogen bonds (Figure 4). However, in contrast to what was found for **9a**·Cl^-, in which each of the four pyrrolic NH protons is hydrogen bonded to the single chloride anion, in the crystal structure of **9a**·NO_3^-, the four pyrrolic NH protons are involved in hydrogen-bonding interactions with only two out of the three nitrate oxygen atoms. In particular, it is seen that one oxygen atom (O2a) is bound to three NH protons (N1H, N2H, and N4H), while another oxygen atom (O1a) is bound to one NH proton (N3H). The N–O distances are in the range of 2.956(2)–3.405(3) Å, the NH proton–oxygen distances are in the range of 2.09(3)–2.56(3) Å, and the N-H-O bond angles are in the range of 159(2)–175(2)°.

A separate important feature of this structure is that it reveals, in conjunction with those for **9a**·2$(CH_3)_2CO$ and **9a**·Cl^-, that macrocycle **9a** may adopt different conformations in the solid state and display different binding modes when interacting with different substrates. This leads us to suggest that **9a** and its congeners could be versatile hosts that might be endowed with a degree of inherent selectivity based on, for example, an ability of certain substrates, solvents, and so forth to modulate their conformational flexibility.

In the case of **10a**, diffraction grade crystals were obtained for the hexafluorophosphate complex, **10a**·PF_6^- (TBA counterion). The corresponding X-ray analysis revealed a structure without any evident symmetry (Figure 5). However, it also revealed that the PF_6^- ion is bound through five well-defined hydrogen bonds involving five out of the six possible pyrrole NH donor groups. The associated NH H–F distances are in the range of 2.38–2.63 Å, and the N-H-F bond angles are in the range of 165.5–173.8°. Other possible hydrogen bonds are also seen involving N6H···F6 and N4H···F1. In this case, the N–F bond lengths, 3.049(12) and 3.318(11) Å, respectively, were found to be within the range expected for these kinds of hydrogen-bonding interactions. However, the corresponding bond angles of 116.7° and 138.1°, respectively, are less than ideal. When the structure is viewed from the perspective of the bound PF_6^- ion, it is seen that four out of the six possible fluorine atoms also participate in binding interactions, as determined from their hydrogen binding parameters. In particular, these latter N–F

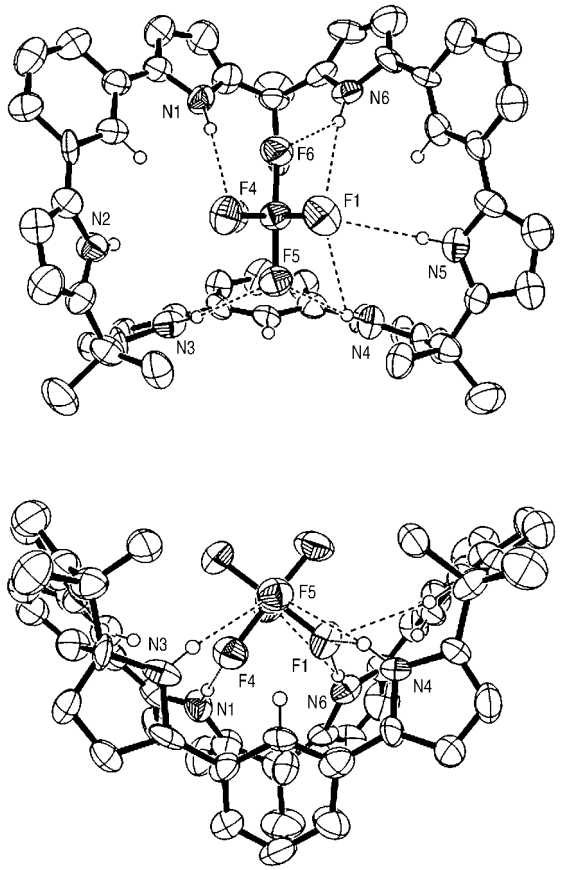

Figure 5. X-ray crystal structure of **10a**·PF_6^- (ORTEP, displacement ellipsoids scaled to the 50% probability level; some hydrogen atoms have been removed for clarity). Top: top view; bottom: side view. Dashed lines are indicative of N–H···F hydrogen bonds.

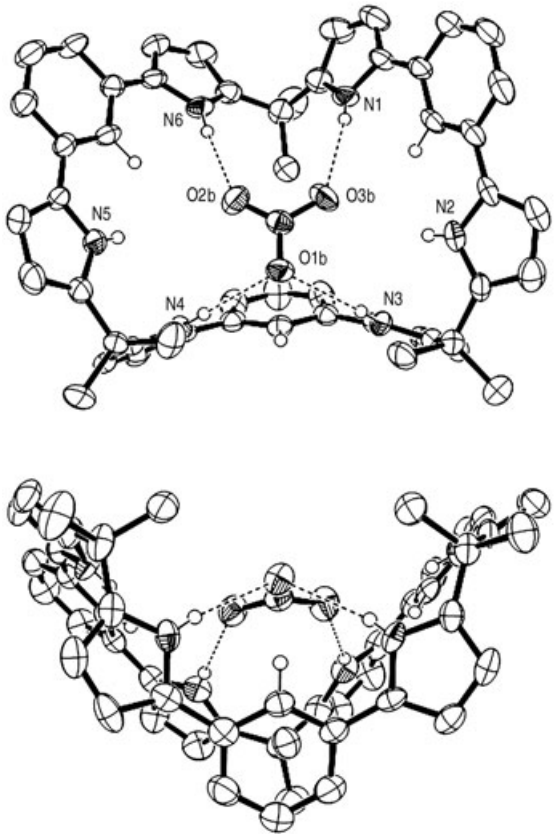

Figure 6. X-ray crystal structure of **10a**·NO_3^- (ORTEP, displacement ellipsoids scaled to the 50% probability level; some hydrogen atoms have been removed for clarity). Top: top view; bottom: side view. Dashed lines are indicative of N–H···O hydrogen bonds.

distances are in the range of 3.263(12)–3.523(12) Å. In contrast to what is seen in the structure of **9a**·2$(CH_3)_2CO$, in the case of **10a**·PF_6^-, the two fluoride atoms participating in the hydrogen bonding interact pairwise with the pyrrole groups attached to the two benzene rings, as opposed to those attached to the bridging, *meso*-like carbon atoms.

Diffraction-grade crystals of **10a**·NO_3^- were obtained by using conditions analogous to those used to obtain crystals of **9a**·NO_3^-. The resulting structure is shown in Figure 6. Here, it is seen that the macrocycle adopts a V-shaped conformation (C_s), with four out of its six pyrrole NH protons bound to a nitrate anion through four NH···O hydrogen bonds. In contrast to what is seen in the case of **9a**·NO_3^-, all three oxygen atoms of the nitrate anion in **10a**·NO_3^- are involved in hydrogen-bonding interactions with the receptor in the solid state. Specifically, these hydrogen bonds include N1–H···O3b, N3–H···O1b, N4–H···O1b, and N6–H···O2b. The two remaining pyrrole units (those containing the N5 and N2 atoms) are not involved in any hydrogen-bonding interactions with the bound anion. The N–O distances are in the range of 3.107(4)–3.304(3) Å, the NH proton–oxygen distances are in the range of 2.32(3)–2.51(2) Å, and the N-H-O bond angles are in the range of 167(3)–172(3)°.

Further comparison of the solid-state molecular structure of **10a**·NO_3^- with that of **10a**·PF_6^- reveals that, in both cases, not all the pyrrole units are involved in hydrogen-bonding interactions with the bound anions. As with the solution phase K_a data given in Table 1, these solid-state structural features are thought to reflect a cavity in **10a** that is less optimized, in terms of size, shape, and perhaps inherent flexibility, for small-anion binding than that present in **9a**.

An X-ray structural analysis of **11a**, studied as **11a**·4$C_4H_8O_2$, revealed that this larger macrocycle adopts a square-shaped conformation (Figure 7). In contrast to the

Table 1. Anion-binding constants [M^{-1}] determined in [D_2]dichloromethane by means of ^{1}H NMR spectroscopic titrations.[a]

	9a	**10a**	**11a**	**1**	**8a**	**16**
F^-	>10000[b]	>10000[b]	n.d.	17000[c]	2300[b]	2100
Cl^-	>10000	3100	>10000	350[c]	4300	110
Br^-	>10000	390	>10000	10[c]	1100	19
I^-	>10000	150	n.d.	<10[c]	190	<10
HSO_4^-	>10000	850	n.d.	<10[c]	290	<10
$H_2PO_4^-$	6300	1700	n.d.	97[c]	1300	310
NO_3^-	>10000	5100	>10000	<10	280	11
ClO_4^-	7900	30	110	n.d.	32	<10

[a] Anion used in the assay were in the form of their tetrabutylammonium salts; n.d. not determinable. [b] Tetrabutylammonium fluoride trihydrate was used as the anion source. [c] From reference [1].

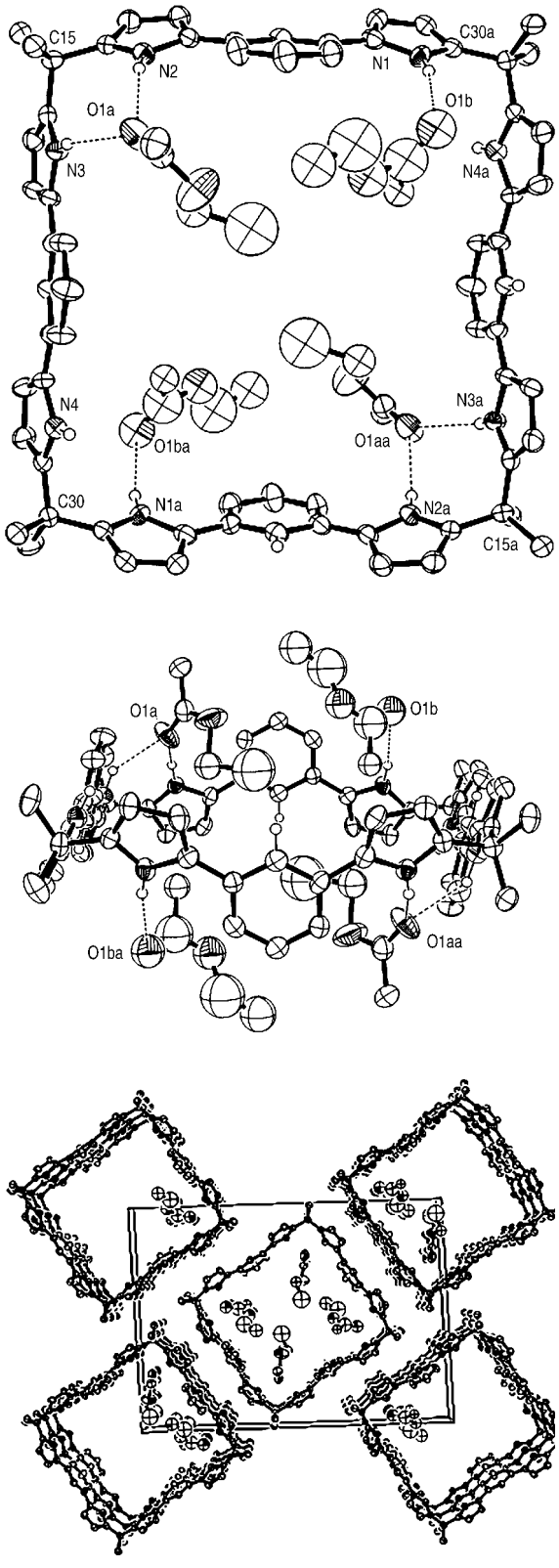

Figure 7. X-ray crystal structure of **11a**·$(C_4H_8O_2)_4$ (ORTEP, displacement ellipsoids scaled to the 30% probability level; some hydrogen atoms omitted for clarity). Top: top view; middle: side view; bottom: unit-cell packing diagram. Dashed lines are indicative of N–H···O hydrogen bonds. The ethyl acetate molecules with atoms O1b, O1ba are hydrogen bonded to a second macrocycle related by a *b* axis translation.

conformation of BPB seen in the solid state (cf. Figure 1), in **11a** each BPB unit adopts a *trans* conformation with both pyrrole units pointing away from the center. The four ethyl acetate molecule interacts with the macrocycle through NH···O (carbonyl) hydrogen bonds. Interestingly, the two pyrrole units attached to the *meso*-carbon C15 (and C15a) are bound to one ethyl acetate molecule through two NH–O hydrogen bonds, while each of the pyrrole units attached to the *meso*-carbon C30 (and C30a) form hydrogen bonds to one ethyl acetate molecule. This last species is also bound to a second pyrrole from another macrocycle. As the result of these interactions, the unit cell packing diagram reveals a columnlike assembly, as can be seen from an inspection of Figure 7 (bottom).

Anion-binding studies: Due to the poor solubility of compound **9a** in acetonitrile and DMSO, preliminary anion-binding studies of compounds **9a**–**11a** were carried out in [D_2]dichloromethane by using standard ^{1}H NMR spectroscopic titration methods. Analogous titrations involving compounds **8a**, **1**, and dimethyldipyrromethane **16** (considered here as the building block for calix[4]pyrrole **1** and thus used for comparison with building block **8a**) were also carried out.

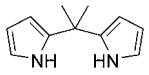

16

In the case of **9a**, the pyrrole NH signals were initially found to broaden beyond the point of clear identification upon the addition of the various halide anions and dihydrogen phosphate anion (these and other anions studied as their TBA salts) before again becoming sharp in the presence of excess anion. Such broadening was also observed for the BPB 2-CH signal in the case of the halides. It was not observed for either signal in the case of HSO_4^-, NO_3^-, and ClO_4^-. Rather, clear shifts in these signals were seen. However, in all cases, substantial shifts for the BPB 2-CH signal in **9a** were seen over the full course of the titration, with downfield shifts ranging between 0.52 and 2.05 ppm, depending on the choice of anion.

In light of the above observations, the change in chemical shift of the pyrrolic NH resonance as a function of anion concentration was used to determine the K_a in the case of HSO_4^-, NO_3^-, and ClO_4^-. By contrast, the changes in either the β-pyrrolic CH or benzene 2-CH resonances were used to follow the binding process in the case of the halides and dihydrogen phosphate, respectively. In all cases, curve fitting was carried out by using standard methods (i.e., as described by Wilcox[18] or Connor;[19] see the Supporting Information).

The anion-binding constants determined in this way for macrocycle **9a** and open-chain control **8a** are given in Table 1, along with those recorded for **1** and **16**. As might be inferred from the broadening of the NH peaks seen in

many of the NMR spectroscopic titrations, compound **9a** was found to be a very effective anion receptor. In fact, with the exception of dihydrogen phosphate and perchlorate, for which K_a values of 6300 and 8400 M^{-1}, respectively, were recorded, in all cases the anion affinities proved too large to measure accurately by standard ^{1}H NMR spectroscopic titration methods. This stands in marked contrast to what is seen in the case of **1**, for which strong binding is seen only in the case of fluoride anion and no appreciable binding is seen in the case of perchlorate. Interestingly, the open-chain control system **8a** was also found to be a more effective anion receptor than **16**, and even macrocycle **1** in some cases, although it was found to be a far less selective receptor than these last two species.

Table 1 also shows that compared to **9a**, the larger macrocyclic receptor **10a** is a less effective anion receptor for almost all anions of interest. This is thought to reflect the destabilizing effects of its large cavity size and relatively rigid structure. Not only is the large cavity size present in **10a** incompatible with the size of most anions of interest, the rather rigid nature of the receptor (close to triangular shape) limits its ability to adopt different conformations suitable for coordinating anions with different sizes and geometries. However, **10a** does show a high affinity for the nitrate anion, traditionally a weak hydrogen-bonding acceptor. This selectivity, we think, reflects the relatively good size and geometry matching between this particular triangular anion and the central core defined by the receptor.

^{1}H NMR spectroscopic titration studies involving compound **11a** failed to provide reliable binding constants for F^-, I^-, HSO_4^-, and $H_2PO_4^-$, due either to loss in the chemical shifts used to follow the anion-binding process (F^-, HSO_4^-, and $H_2PO_4^-$) or difficulties in fitting the binding profile curve (I^-) using standard curve fitting methods. However, with the exception of ClO_4^-, for the other anions of interest (Cl^-, Br^-, and NO_3^-) **11a** shows higher binding affinities than **10a**. Compound **11a** has larger apparent core size than either **10a** or **9a**, a feature that should make it even less compatible with most anions, than either **10a** or **9a**. However, macrocycle **11a** is more flexible than either macrocycle **10a** or **9a**; this flexibility may allow it to "mold itself" to various anions. To the extent this occurs, higher, rather than lower, anion affinities would be in fact expected.

Because of the limitations inherent in NMR-spectroscopy-based titrations, efforts were made to determine the anion affinities of these compounds by means of other, more sensitive methods. Unfortunately, the lack of a spectroscopic "handle" in **9a**–**11a** meant that no useful binding information could be obtained from UV-visible or fluorescence titration experiments. On the other hand, it was found that reliable isothermal titration calorimetry (ITC) measurements could be carried out in 1,2-dichloroethane.

Table 2 shows the binding constants for compounds **8a**–**11a**, and **1** with Cl^-, Br^-, HSO_4^-, and NO_3^- ions. Compound **9a** has the highest anion affinities for all four anions relative to the other anion receptors. However, it lacks good selectivity. For example, in the case of chloride, it is seen that **9a** binds chloride anion with a 1:1 affinity constant, K_a, of 5.6×10^6 M^{-1}, or roughly 300 times as well as **1** under analogous conditions ($K_a=1.8\times10^4$ M^{-1}). In contrast to what might be inferred from the NMR studies carried out in dichloromethane, analogous ITC studies involving **8a** revealed that this open-chain control system binds chloride anion less effectively than **1** in 1,2-dichloroethane (DCE) ($K_a=6.8\times10^3$ vs. 1.8×10^4 M^{-1} for **8a** and **1**, respectively). Surprisingly, **9a** binds the bromide anion even more strongly than the chloride anion, a phenomenon that is rarely seen in the calixpyrrole-type anion receptors. This enhanced affinity for Br^- over Cl^- displayed by **9a**, we think, is a direct reflection of the fact that the receptor cavity present in **9a** provides a better size match for this larger halide anion and that this compatibility is sufficient to overcome any inherent binding differences due to charge density or purely electrostatic effects.

Table 2. Anion-binding constants measured by ITC titration method in 1,2-dichloroethane.[a]

	9a	**10a**	**11a**	**1**	**8a**
Cl^-	5600000	82000	240000	18000	6800
Br^-	21000000	5600	44000	n.d.	3300
HSO_4^-	1200000	11000	76000	n.d.	n.d.
NO_3^-	2500000	3800	220000	n.d.	n.d.

[a] Anion used in the assay were in the form of their tetrabutylammonium salts; n.d. not determinable.

Compound **10a** displays selectivity for Cl^- over Br^-, HSO_4^-, and NO_3^- as determined by ITC in dichloroethane. This stands in contrast to what is inferred from ^{1}H NMR spectroscopic titrations carried out in dichloromethane, in which selectivity towards NO_3^- was observed. The difference between what is seen by ITC in dichloroethane and by ^{1}H NMR spectroscopic titration in dichloromethane provides a cogent reminder of the fact that the anion-binding properties (absolute affinities; relative selectivities) of an anion receptor can be substantially different in different solvent media.[1,20] There are a number of factors that could account for this, including differences in ion pairing in both the product and the initial anion–cation salt, as well as the fact that these two methods probe different chemistries (e.g., interactions with pyrrolic NH protons vs. overall system thermodynamics). Such concerns aside, it is important to appreciate that the basic conclusion, namely that **10a** is a less effect anion receptor than **9a**, still stands.

Compound **11a** also displays higher anion affinities than **10a**. However, it binds most test anions more weakly than **9a**. Compounds **9a**–**11a** all display stronger anion-binding affinities than **1**, and their building block **8a**. Compound **8a** also displayed a greater propensity to bind anions than **16**, a species that displayed no evidence of anion binding under the conditions of the present ITC studies. These findings are consistent with the results from ^{1}H NMR titration studies.

The ITC studies serve to highlight further the fact that, under identical conditions of measurement, macrocycle **9a** is a far more effective anion receptor than calix[4]pyrrole **1**. This difference is notable, since they both possess the same

number of potential NH hydrogen-bond donor groups (four in both cases). One potential explanation lies in the fact that the basic subunit present in **9a**, namely 1,3-bis(pyrrol-2-yl)-benzene (**8a**), displays a higher inherent anion affinity than the corresponding "building block" present in calix[4]pyrrole **1**, namely dimethyldipyrromethane (**16**). For example, this latter species fails to show evidence of anion binding by ITC and gives rise to only a modest K_a (ca. $110\,M^{-1}$) for chloride in [D_2]dichloromethane, as determined from standard ^{1}H NMR titration methods. It is thus clearly a very weak stand-alone anion receptor. By contrast, compound **8a** displays a high affinity not only for chloride, but also demonstrates some degree of affinity for most of the anions tested by ^{1}H NMR titration (cf. Table 1).

Presumably, the large disparity in chloride anion affinity observed for these two bis-pyrrole fragments reflects the fact that the bite angle present in **8a** provides a better structural match to chloride (and likely most other anions) than does dimethyldipyrromethane. However, electronic effects could also contribute, due to the presence of the benzene ring and the CH–anion interaction involving the 2-position of this bridging group.

Many of these same effects are expected to be important in the case of the macrocyclic system **9a**, with the importance of the CH–anion hydrogen-bonding interactions being specifically inferred from both the solid-state structural analysis of **9a**·Cl^- (Figure 3) and the changes in the chemical shifts seen in the NMR titrations (vide supra). However, in the case of the macrocycle, conformational effects are also likely to play a greater role than in the case of the corresponding open-chain systems. Here, it is specifically proposed that the larger nature of the BPB fragment present in **9a** and the presence of two bridging phenyl groups that can rotate rather freely allows it to adopt more readily conformations favorable to the complexation of most anions, including specifically the chloride anion.

Conclusion

In conclusion, we have synthesized three new calixpyrrole-like macrocycles, namely **9–11**, from an easy-to-synthesize building block, BPB **8**, which serves as a structural surrogate for terpyrrole. Anion-binding studies carried out in dichloromethane and dichloroethane confirm that compound **9a** is a versatile anion receptor, binding most anions, including chloride, with affinities that are greatly enhanced relative to those of **1**. Such observations are rationalized in terms of the presence of a "building block", BPB **8a**, which displays a higher inherent affinity for anions than does dimethyldipyrromethane **16**, the analogous core subunit present in calix[4]pyrrole **1**. The ability to more readily adopt conformations that are suitable for anion binding is also considered important, especially in the case of the larger system **11a**. Current work is focused on preparing new systems that will allow the interplay of these various influencing factors to be better understood.

Experimental Section

Tetrabutylammonium chloride was dried under vacuum at 40 °C for 24 h before use. Dichloromethane was dried by distillation under argon over calcium hydride. Tetrahydrofuran (THF) was dried by passage through two columns of activated alumina. [D_2]Dichloromethane was purchased in individual ampoules from Cambridge Isotope Inc. and used without further purification or drying. All other reagents were obtained from commercial sources and used as received. Melting points were measured on a Mel-Temp II device and not corrected. ^{1}H and ^{13}C NMR spectra used in the characterization of product and titration studies were recorded on Varian Unity 400 MHz spectrometers. Low-resolution FAB and CI mass spectra were obtained on a Finningan MAT TSQ 70 mass spectrometer. High-resolution FAB and CI mass spectra were obtained on a VG ZAB2-E mass spectrometer.

***N*,*N*′-Diallylisophthaldiamide (12a)**: Allylamine (12.56 g, 0.22 mol) and triethylamine (30.36 g, 0.3 mol) were dissolved in dichloromethane (100 mL) in a 500 mL round-bottomed flask equipped with a 250 mL addition funnel and cooled with an ice–water bath. Isophthaloyl chloride (**13**; 20.30 g, 0.1 mol) dissolved in dichloromethane (100 mL) was then added dropwise through an addition funnel to the amine solution. Once the addition was complete, the cooling bath was removed and the reaction was stirred at room temperature overnight. The reaction mixture was washed with water (3×100 mL) and brine (100 mL), and dried with sodium sulfate. The volatile components were removed using a rotary evaporator and the residue was dried under vacuum. The resulting pale yellow solid (23.15 g, 95 %) was used for the next step without further purification. M.p. 115 °C; ^{1}H NMR (400 MHz, [D_1]chloroform, 25 °C): δ = 4.08 (m, 4H; NHCH_2), 5.19 (dd, J = 1.2, 10 Hz, 2H; C=CH*H cis*), 5.26 (dd, J = 1.2, 17.2 Hz, 2H; C=C*H*H *trans*), 5.92 (m, 2H; C*H*=CH_2), 6.47 (s, 2H; NH), 7.51 (t, J = 8 Hz, 1H; benzene CH), 7.94 (dd, J = 2, 8 Hz, 2H; benzene CH), 8.22 ppm (t, J = 2 Hz, 1H; benzene CH); ^{13}C NMR (100 MHz, [D_1]chloroform, 25 °C): δ = 42.53, 116.92, 125.33, 128.95, 130.02, 133.74, 134.65, 166.50 ppm; HRMS (CI^+): *m*/*z* calcd for $C_{14}H_{17}N_2O_2$ [*M*+H]$^+$: 245.1290; found: 245.1292.

***N*,*N*′-Diallyl-5-(*tert*-butyl)isophthaldiamide (12b)**: A mixture of 5-(*tert*-butyl)isophthalic acid (11.10 g, 50 mmol), thionyl chloride (150 mL), and ten drops of DMF was heated under refulx for 5 h. Excess thionyl chloride was removed under vacuum to give 5-(*tert*-butyl)isophthaloyl chloride (**14**), which was used directly in the next step without purification. Allylamine (6.28 g, 0.11 mol) and triethylamine (12.12 g, 0.12 mol) were dissolved in dichloromethane (100 mL) in a 500 mL round-bottomed flask equipped with a 250 mL addition funnel and cooled with ice–water bath. 5-(*tert*-Butyl)isophthaloyl dichloride (excess) dissolved in dichloromethane (100 mL) was then added dropwise through the funnel to the amine solution. Once the addition was complete, the cooling bath was removed and the reaction was stirred at room temperature overnight. The reaction mixture was washed with water (3×100 mL) and brine (100 mL), and dried with sodium sulfate. The volatile components were removed using a rotary evaporator, and the residue was dried under vacuum. The resulting pale yellow solid (15 g, quantitative) was used for the next step without further purification. M.p. 139 °C; ^{1}H NMR (400 MHz, [D_1]chloroform, 25 °C): δ = 1.31 (s, 9H; CH_3), 4.04 (m, 4H; NHCH_2), 5.14 (dd, J = 1.2, 10 Hz, 2H; C=CH*H* cis), 5.22 (dd, J = 1.2, 16.8 Hz, 2H; C=C*H*H *trans*), 5.88 (m, 2H; C*H*=CH_2), 6.54 (s, 2H; NH), 7.94 (d, J = 1.6 Hz, 2H; benzene CH), 7.92 ppm (t, J = 1.6, 2H; benzene CH); ^{13}C NMR (100 MHz, [D_1]chloroform, 25 °C): δ = 31.16, 35.05, 42.57, 116.92, 122.21, 127.29, 133.87, 134.50, 152.58, 167.00 ppm; HRMS (CI^+): *m*/*z* calcd for $C_{18}H_{25}N_2O_2$ [*M*+H]$^+$: 301.1916; found: 301.1920.

***N*,*N*′-Diallyl-5-hexyloxyisophthaldiamide (12c)**: Dimethyl-5-hexyloxyisophthalate (**15**; 8.82 g, 30 mmol) was dissolved in allylamine (90 mL), and the mixture was stirred at RT for 4 days. The excess solvent was removed under reduced pressure. Column chromatographic purification (silica gel, 1 % CH_3OH in dichloromethane, eluent) of the residue afforded **12c** in the form of a brown oil (9 g, 75 %). ^{1}H NMR (400 MHz, [D_1]chloroform, 25 °C): δ = 0.91 (t, J = 7.2 Hz, 3H; CH_3), 1.33 (m, 4H; CH_2), 1.45 (m, 2H; CH_2), 1.78 (m, 2H; CH_2), 4.01 (t, J = 6.4 Hz, 2H; OCH_2), 4.06 (m, 4H; NHCH_2), 5.18 (dd, J = 1.2, 10 Hz, 2H; C=CH*H*

cis), 5.25 (dd, $J=1.2$, 16.8 Hz, 2H; C=C*H*H *trans*), 5.91 (m, 2H; C*H*=CH_2), 6.46 (s, 2H; NH), 7.45 (d, $J=2.0$ Hz, 2H; benzene CH), 7.73 ppm (t, $J=1.2$ Hz, 2H; benzene CH); ^{13}C NMR (100 MHz, [D$_1$]chloroform, 25°C): $\delta=14.00$, 22.55, 26.00, 29.03, 31.47, 42.55, 68.57, 116.12, 116.89, 116.99, 133.73, 136.01, 159.57, 166.38 ppm; HRMS (CI$^+$): *m*/*z* calcd for $C_{20}H_{29}N_2O_3$ [*M*+H]$^+$: 345.2178; found: 345.2181.

1,3-Bis(pyrrol-2-yl)benzene (8a): A mixture of **12a** (2.44 g, 10 mmol), phosgene (20% solution in toluene, 40 mL), and DMF (4 drops) was stirred for 15 h at room temperature under Ar. The resulting mixture was then heated at 40–45°C for 2 h, after which the solvent was removed in vacuo (caution: phosgene is highly toxic and must be handled with appropriate care. Two cold traps immersed in liquid N_2 were used to receive the solvent and phosgene). The residue was dissolved in THF (60 mL) and added dropwise with stirring to a solution of potassium *tert*-butoxide (5.89 g, 52 mmol) in THF (60 mL) at 5–10°C under Ar. After stirring for 1 h at this temperature, the reaction mixture was poured into ice water and extracted with chloroform (3×100 mL). The organic phase was dried (Na_2SO_4) and evaporated to dryness. The residue was subjected to column chromatography (silica gel, dichloromethane, eluent) to give crude product, which upon recrystallization from dichloromethane/hexanes afforded **8a** in the form of a white solid (0.6 g, 29%). M.p. 163°C; ^{1}H NMR (400 MHz, [D$_1$]chloroform, 25°C): $\delta=6.32$ (q, $J=2.8$ Hz, 2H; pyrrole CH), 6.56 (m, 2H; pyrrole CH), 6.89 (m, 2H; pyrrole CH), 7.30–7.39 (m, 3H; benzene CH), 7.58 (t, $J=1.6$ Hz, 1H; benzene CH), 8.47 ppm (brs, 2H; pyrrole NH); ^{13}C NMR (100 MHz, [D$_1$]chloroform, 25°C): $\delta=100.18$, 110.16, 118.98, 119.62, 121.77, 129.40, 131.95, 133.36 ppm; HRMS (CI$^+$): *m*/*z* calcd for $C_{14}H_{13}N_2$ [*M*+H]$^+$: 209.1079; found: 209.1079.

5-(*tert*-Butyl)-1,3-bis(pyrrol-2-yl)benzene (8b): Compound **8b** was prepared from **12b** (3 g, 10 mmol) in the same manner as **8a**. After column chromatography (silica gel, dichloromethane/hexanes 4:1, eluent), the crude product was recrystalized from benzene/hexanes to afford **8b** in the form of a pale yellow solid (1.13 g, 43%). M.p. 163°C; ^{1}H NMR (400 MHz, [D$_1$]chloroform, 25°C): $\delta=1.37$ (s, 9H; CH_3), 6.32 (m, 2H; pyrrole CH), 6.54 (m, 2H; pyrrole CH), 6.88 (m, 2H; pyrrole CH), 7.4 (d, $J=1.2$ Hz, 2H; benzene CH), 7.38 (t, $J=1.2$ Hz, 1H; benzene CH), 8.47 ppm (brs, 2H; pyrrole NH); ^{13}C NMR (100 MHz, [D$_1$]chloroform, 25°C): $\delta=31.33$, 34.81, 106.03, 110.06, 117.44, 118.73, 119.40, 132.50, 133.14, 152.30 ppm; HRMS (CI$^+$): *m*/*z* calcd for $C_{18}H_{21}N_2$ [*M*+H]$^+$: 265.1705; found: 265.1700.

5-Hexyloxy-1,3-bis(pyrrol-2-yl)benzene (8c): This compound was prepared from **12c** (5 g, 14.5 mmol) in the same manner as **8a**. Column chromatography (silica gel, dichloromethane/hexanes 1:1, eluent) afforded **8c** in the form of a pale yellow solid (3.30 g, 96%). M.p. 66°C; ^{1}H NMR (400 MHz, [D$_1$]chloroform, 25°C): $\delta=0.91$ (t, $J=6.8$ Hz, 3H; CH_3), 1.36 (m, 4H; CH_2), 1.49 (m, 2H; CH_2), 1.81 (m, 2H; CH_2), 4.02 (t, $J=6.4$ Hz, 2H; OCH_2), 6.31 (m, 2H; pyrrole CH), 6.54 (m, 2H; pyrrole CH), 6.85 (d, $J=1.2$ Hz, 2H; benzene CH), 6.87 (m, 2H; pyrrole CH), 7.16 (t, $J=1.2$ Hz, 1H; benzene CH), 8.45 ppm (brs, 2H; pyrrole NH); ^{13}C NMR (100 MHz, [D$_1$]chloroform, 25°C): $\delta=14.03$, 22.60, 25.73, 29.27, 31.57, 68.11, 106.31, 108.16, 110.07, 112.33, 118.91, 131.96, 134.55, 160.01 ppm; HRMS (CI$^+$): *m*/*z* calcd for $C_{20}H_{25}N_2O$ [*M*+H]$^+$: 309.1967; found: 309.1967.

Calix[*n*]1,3-bis(pyrrol-2-yl)benzenes 9a–11a: Compound **8a** (0.42 g, 2 mmol) was dissolved in acetone (40 mL) and the mixture was degassed by bubbling with Ar for ten minutes. Trifluoroacetic acid (0.23 g, 2 mmol) was added, and the resulting mixture was stirred at room temperature for 12 h. Triethylamine was added to quench the reaction, and the solvent was evaporated in vacuo. Column chromatography (silica gel, gradient of hexanes to hexanes/ethyl acetate 1:9 as eluents) afforded the title compounds **9a–11a**:

Compound 9a: White solid (68 mg, 14%); m.p. >180°C (decomp); ^{1}H NMR (400 MHz, [D$_1$]chloroform, 25°C): $\delta=1.74$ (s, 12H; CH_3), 6.17 (t, $J=2.8$ Hz, 4H; β-pyrrole CH), 6.37 (t, $J=2.8$ Hz, 4H; β-pyrrole CH), 7.20 (s, 2H; benzene CH), 7.35 (s, 6H; benzene CH), 8.09 ppm (s, 4H; pyrrole NH); ^{13}C NMR (100 MHz, [D$_1$]chloroform, 25°C): $\delta=30.13$, 35.81, 106.14, 107.32, 120.14, 124.88, 129.56, 131.54, 134.02, 140.27 ppm; HRMS (CI$^+$): *m*/*z* calcd for $C_{34}H_{33}N_4$ [*M*+H]$^+$: 497.2705; found: 497.2700.

Compound 10a: White solid (82 mg, 17%); m.p. >140°C (decomp); ^{1}H NMR (400 MHz, [D$_1$]chloroform, 25°C): $\delta=1.72$ (s, 18H; CH_3), 6.20 (t, $J=2.8$ Hz, 6H; β-pyrrole CH), 6.40 (t, $J=2.8$ Hz, 6H; β-pyrrole CH), 7.15–7.24 (m, 12H; benzene CH), 7.96 ppm (s, 6H; pyrrole NH); ^{13}C NMR (100 MHz, [D$_1$]chloroform, 25°C): $\delta=29.29$, 35.73, 105.80, 105.89, 118.51, 121.55, 129.21, 131.53, 132.96, 140.08 ppm; HRMS (CI$^+$): *m*/*z* calcd for $C_{51}H_{49}N_6$ [*M*+H]$^+$: 745.4019; found: 745.4028.

Compound 11a: White solid (64 mg, 13%); m.p. >140°C (decomp.); ^{1}H NMR (400 MHz, [D$_1$]chloroform, 25°C): $\delta=1.70$ (s, 24H; CH_3), 6.17 (t, $J=2.8$ Hz, 8H; β-pyrrole CH), 6.41 (t, $J=2.8$ Hz, 8H; β-pyrrole CH), 7.15–7.23 (m, 12H; benzene CH), 7.33 (t, $J=1.2$ Hz, 4H; benzene CH), 8.03 ppm (m, 8H; pyrrole NH); ^{13}C NMR (100 MHz, [D$_1$]chloroform, 25°C): $\delta=29.26$, 35.70, 105.83, 105.88, 118.97, 121.45, 129.19, 131.43, 133.05, 140.06 ppm; HRMS (CI$^+$): *m*/*z* calcd for $C_{68}H_{65}N_8$ [*M*+H]$^+$: 993.5332; found: 993.5304.

Calix[*n*]5-(*tert*-butyl)-1,3-bis(pyrrol-2-yl)benzene (9b–11b): This set of compounds was prepared from **8b** (0.26 g, 1 mmol) in a manner analogous to that used to prepare **9a–11a**. Column chromatography (silica gel, gradient of hexanes to hexanes/ethyl acetate 1:9 as eluent) afforded **9b–11b**:

Compound 9b: White solid (50 mg, 16%); m.p. >200°C (decomp); ^{1}H NMR (400 MHz, [D$_1$]chloroform, 25°C): $\delta=1.34$ (s, 18H; benzene CH_3), 1.72 (s, 12H; meso CH_3), 6.17 (t, $J=2.8$ Hz, 4H; β-pyrrole CH), 6.37 (t, $J=2.8$ Hz, 4H; β-pyrrole CH), 7.03 (t, $J=1.6$ Hz, 2H; benzene CH), 7.40 (d, $J=1.6$ Hz, 4H; benzene CH), 8.08 ppm (s, 4H; pyrrole NH); ^{13}C NMR (100 MHz, [D$_1$]chloroform, 25°C): $\delta=30.34$, 31.24, 34.77, 35.87, 105.96, 106.86, 118.15, 122.54, 132.02, 133.84, 134.00, 152.56 ppm; HRMS (CI$^+$): *m*/*z* calcd for $C_{42}H_{49}N_4$ [*M*+H]$^+$: 609.3957; found: 609.3966.

Compound 10b: White solid (66 mg, 22%); m.p. 194°C (decomp); ^{1}H NMR (400 MHz, [D$_1$]chloroform, 25°C): $\delta=1.30$ (s, 27H; benzene CH_3), 1.73 (s, 18H; meso CH_3), 6.20 (t, $J=2.8$ Hz, 6H; β-pyrrole CH), 6.39 (t, $J=2.8$ Hz, 6H; β-pyrrole CH), 7.07 (t, $J=1.2$ Hz, 3H; benzene CH), 7.21 (d, $J=1.2$ Hz, 6H; benzene CH), 8.03 ppm (s, 6H; pyrrole NH); ^{13}C NMR (100 MHz, [D$_1$]chloroform, 25°C): $\delta=29.43$, 31.26, 34.71, 35.75, 105.68, 105.80, 116.37, 119.17, 131.99, 132.72, 139.89, 152.11 ppm; HRMS (CI$^+$): *m*/*z* calcd for $C_{63}H_{73}N_6$ [*M*+H]$^+$: 913.5897; found: 913.5912.

Compound 11b: White solid (34 mg, 11%); m.p. >180°C; ^{1}H NMR (400 MHz, [D$_1$]chloroform, 25°C): $\delta=1.29$ (s, 36H; benzene CH_3), 1.70 (s, 24H; meso CH_3), 6.15 (t, $J=2.8$ Hz, 8H; β-pyrrole CH), 6.38 (t, $J=2.8$ Hz, 8H; β-pyrrole CH), 7.11 (t, $J=1.2$ Hz, 4H; benzene CH), 7.19 (d, $J=1.2$ Hz, 8H; benzene CH), 8.04 ppm (s, 8H; pyrrole NH); ^{13}C NMR (100 MHz, [D$_1$]chloroform, 25°C): $\delta=29.30$, 31.26, 34.70, 35.70, 105.76, 116.78, 119.35, 131.98, 132.91, 139.90, 152.10 ppm; HRMS (CI$^+$): *m*/*z* calcd for $C_{84}H_{97}N_8$ [*M*+H]$^+$: 1217.7836; found: 1217.7833.

Calix[*n*][5-hexyloxy-1,3-bis(pyrrol-2-yl)benzene] (9c–11c): This set of compounds was prepared from **7c** (0.46 g, 1.5 mmol) by using the same procedure as used to prepare **9a–11a**. Column chromatography (silica gel, gradient of hexanes to hexanes/ethyl acetate 1:19 as eleuent) afforded **9c–11c**:

Compound 9c: White solid (58 mg, 11%); m.p. 172°C; ^{1}H NMR (400 MHz, [D$_1$]chloroform, 25°C): $\delta=0.90$ (t, $J=6.8$ Hz, 6H; CH_2CH_3), 1.34 (m, 8H; CH_2), 1.46 (m, 4H; CH_2), 1.72 (s, 12H; meso CH_3), 1.79 (m, 4H; CH_2), 3.99 (t, $J=6.8$ Hz, 4H; OCH_2), 6.16 (t, $J=2.8$ Hz, 4H; β-pyrrole CH), 6.36 (t, $J=2.8$ Hz, 4H; β-pyrrole CH), 6.80 (t, $J=1.2$ Hz, 2H; benzene CH), 6.90 (d, $J=1.2$ Hz, 4H; benzene CH), 8.10 ppm (s, 4H; pyrrole NH); ^{13}C NMR (100 MHz, [D$_1$]chloroform, 25°C): $\delta=14.03$, 22.60, 25.70, 29.20, 30.17, 31.56, 35.80, 68.10, 106.07, 107.28, 111.01, 112.72, 131.60, 135.28, 140.14, 159.93 ppm; HRMS (CI$^+$): *m*/*z* calcd for $C_{46}H_{57}N_4O_2$ [*M*+H]$^+$: 697.4482; found: 697.4482.

Compound 10c: White solid (104 mg, 20%); m.p. >80°C (no clear m.p.); ^{1}H NMR (400 MHz, [D$_1$]chloroform, 25°C): $\delta=0.89$ (t, $J=6.8$ Hz, 9H; CH_2CH_3), 1.31 (m, 12H; CH_2), 1.44 (m, 6H; CH_2), 1.71 (s, 18H; *meso* CH_3), 1.75 (m, 6H; CH_2), 3.95 (t, $J=6.4$ Hz, 6H; OCH_2), 6.18 (t,

$J=2.8$ Hz, 6H; β-pyrrole CH), 6.38 (t, $J=2.8$ Hz, 6H; β-pyrrole CH), 6.69 (d, $J=1.6$ Hz, 6H; benzene CH), 6.83 (t, $J=1.6$ Hz, 3H; benzene CH), 7.93 ppm (s, 6H; pyrrole NH); ^{13}C NMR (100 MHz, [D$_1$]chloroform, 25 °C): $\delta=14.03$, 22.57, 25.70, 29.26, 29.29, 31.56, 35.71, 68.01, 105.86, 105.96, 107.77, 111.44, 131.54, 134.19, 140.00, 159.80 ppm; HRMS (FAB$^+$): m/z calcd for $C_{69}H_{84}N_6O_3$ $[M]^+$: 1044.6605, found: 1044.6631.

Compound 11c: White solid (34 mg, 11%); m.p. >120 °C (no clear m.p.); ^{1}H NMR (400 MHz, [D$_1$]chloroform, 25 °C): $\delta=0.89$ (t, $J=6.8$ Hz, 12H; CH_2CH_3), 1.32 (m, 16H; CH_2), 1.43 (m, 8H; CH_2), 1.69 (s, 24H; meso CH_3), 1.75 (m, 8H; CH_2), 3.94 (t, $J=6.4$ Hz, 8H; OCH_2), 6.13 (t, $J=2.8$ Hz, 8H; β-pyrrole CH), 6.38 (t, $J=2.8$ Hz, 4H; β-pyrrole CH), 6.69 (d, $J=1.2$ Hz, 8H; benzene CH), 6.90 (s, 4H; benzene CH), 8.02 ppm (s, 8H; pyrrole NH); ^{13}C NMR (100 MHz, [D$_1$]chloroform, 25 °C): $\delta=14.03$, 22.57, 25.71, 29.26, 31.57, 35.67, 68.03, 105.83, 106.10, 107.87, 111.80, 131.44, 1354.35, 139.99, 159.82 ppm; HRMS (FAB$^+$): m/z calcd for $C_{92}H_{112}N_8O_4$ $[M]^+$: 1392.8807; found: 1392.8788.

X-ray structure determinations: The data were collected on a Nonius Kappa CCD diffractometer using a graphite monochromator with $Mo_{K\alpha}$ radiation ($\lambda=0.71073$ Å). The data were collected at 153 K by using an Oxford Cryostream low-temperature device. Data reduction were performed using DENZO-SMN.[21] The structures were solved by direct methods using SIR92[22] or SIR97,[23] and refined by full-matrix least-squares on F^2 with anisotropic displacement parameters for the non-H atoms by using SHELXL-97.[24] The hydrogen atoms on carbon were calculated in ideal positions with isotropic displacement parameters set to 1.2 U_{eq} of the attached atom (1.5 U_{eq} for methyl hydrogen atoms). Neutral atom scattering factors and values used to calculate the linear absorption coefficient are from the International Tables for X-ray Crystallography (1992).[25]

Compound 8a: $C_{14}H_{12}N_2$; crystals grew as large thin plates with a slight violet tinge by slow evaporation of a solution of **8a** dissolved in dichloromethane in an atmosphere saturated with hexanes. The data crystal was cut from a larger crystal and had approximate dimensions; $0.27\times0.17\times0.09$ mm: orthorhombic, space group $Pnma$, $a=6.4010(2)$, $b=23.0270(6)$, $c=7.2189(2)$ Å, $\alpha=\beta=\gamma=90°$, $V=1064.04(5)$ Å^3, $Z=4$, $\rho_{calcd}=1.300$ g cm^{-3}, $\mu=0.078$ mm^{-1}, $F(000)=440$. A total of 412 frames of data were collected using ω-scans with a scan range of 1° and a counting time of 129 seconds per frame. A total of 2206 reflections were measured, 1250 of which were unique ($R_{int}=0.0410$). The structure was refined on F^2 to 0.129, with $R(F)$ equal to 0.0550 and a goodness of fit $S=1.14$.

Compound 9a·2C$_3$H$_6$O: $C_{40}H_{44}N_4O_2$; crystals grew as colorless lathes by slow evaporation of a solution of **9a** dissolved in dichloromethane and acetone in an atmosphere saturated with hexanes. The data crystal was cut from a larger crystal and had approximate dimensions; $0.20\times0.20\times0.08$ mm: orthorhombic, space group $P2_12_12_1$, $a=7.25800(10)$, $b=21.3115(4)$, $c=21.5388(4)$ Å, $\alpha=\beta=\gamma=90°$, $V=3331.60(10)$ Å^3, $Z=4$, $\rho_{calcd}=1.222$ g cm^{-3}, $\mu=0.076$ mm^{-1}, $F(000)=1312$. A total of 280 frames of data were collected using ω-scans with a scan range of 1° and a counting time of 190 seconds per frame. A total of 7584 reflections were measured, 4315 of which were unique ($R_{int}=0.0672$). The structure was refined on F^2 to 0.0924, with $R(F)$ equal to 0.0455 and a goodness of fit $S=1.00$.

Compound 9a·C$_{16}$H$_{36}$NCl: $C_{50}H_{68}ClN_5$; crystals grew as pale brown or very light tan plates by slow evaporation of a solution of **9a** and tetrabutylammonium chloride (1:1) dissolved in dichloromethane in an atmosphere saturated with hexanes. The data crystal was cut from a large cluster of crystals and had approximate dimensions $0.43\times0.21\times0.12$ mm: orthorhombic, space group $Pbcn$, $a=41.0311(5)$, $b=12.6474(1)$, $c=17.3594(2)$ Å, $\alpha=\beta=\gamma=90°$, $V=9008.43(17)$ Å^3, $Z=8$, $\rho_{calcd}=1.142$ g cm^{-3}, $\mu=0.124$ mm^{-1}, $F(000)=3360$. A total of 913 frames of data were collected using ω-scans with a scan range of 0.6° and a counting time of 78 seconds per frame. A total of 18826 reflections were measured, 10137 of which were unique ($R_{int}=0.1062$). The structure was refined on F^2 to 0.154, with $R(F)$ equal to 0.0607 and a goodness of fit $S=1.06$.

Compound 9a·C$_{16}$H$_{36}$NNO$_3$: $C_{50}H_{68}N_6O_5$; crystals grew as colorless plates by slow evaporation of a solution of **9a** and tetrabutylammonium nitrate (1:1) dissolved in dichloromethane in an atmosphere saturated with hexanes. The data crystal was cut from a large cluster of crystals and had approximate dimensions $0.51\times0.16\times0.08$ mm: orthorhombic, space group $Pbcn$, $a=40.79880(10)$, $b=12.5954(2)$, $c=17.7740(6)$ Å, $\alpha=\beta=\gamma=90°$, $V=9133.7(3)$ Å^3, $Z=8$, $\rho_{calcd}=1.165$ g cm^{-3}, $\mu=0.073$ mm^{-1}, $F(000)=3472$. A total of 494 frames of data were collected using ω-scans with a scan range of 0.7° and a counting time of 108 seconds per frame. A total of 18428 reflections were measured, 10412 of which were unique ($R_{int}=0.1244$). The structure was refined on F^2 to 0.126, with $R(F)$ equal to 0.0676 and a goodness of fit $S=1.21$.

Compound 10a·C$_{16}$H$_{36}$NPF$_6$·3CH$_2$Cl$_2$: $C_{70}H_{86}Cl_6F_6N_7P$; crystals grew as colorless lathes by slow evaporation of a solution of **10a** and tetrabutylammonium hexafluorophosphate (1:1) dissolved in dichloromethane in an atmosphere saturated with hexanes. The data crystal was a long lathe that had approximate dimensions; $0.56\times0.24\times0.07$ mm: monoclinic, space group $P2_1/c$, $a=19.570(2)$, $b=17.228(2)$, $c=21.934(3)$ Å, $\alpha=\gamma=90°$, $\beta=104.622(4)°$, $V=7155.6(15)$ Å^3, $Z=4$, $\rho_{calcd}=1.228$ g cm^{-3}, $\mu=0.323$ mm^{-1}, $F(000)=2920$. A total of 300 frames of data were collected using ω-scans with a scan range of 1° and a counting time of 169 seconds per frame. A total of 12703 reflections were measured, 7963 of which were unique ($R_{int}=0.1369$). The structure was refined on F^2 to 0.199, with $R(F)$ equal to 0.154 and a goodness of fit $S=1.61$.

Compound 10a·C$_{16}$H$_{36}$NNO$_3$·3CH$_2$Cl$_2$: $C_{70}H_{90}Cl_6N_8O_3$; crystals grew as pale yellow plates by slow evaporation of a solution of **10a** and tetrabutylammonium nitrate (1:1) dissolved in dichloromethane in an atmosphere saturated with hexanes. The data crystal was cut from a cluster of crystals and had approximate dimensions; $0.30\times0.24\times0.17$ mm: monoclinic, space group $P2_1/c$, $a=18.6292(3)$, $b=16.9861(3)$, $c=22.4638(4)$ Å, $\alpha=\gamma=90°$, $\beta=102.662(1)°$, $V=6935.5(2)$ Å^3, $Z=4$, $\rho_{calcd}=1.249$ g cm^{-3}, $\mu=0.299$ mm^{-1}, $F(000)=2768$. A total of 304 frames of data were collected using ω-scans with a scan range of 1° and a counting time of 217 seconds per frame. A total of 27570 reflections were measured, 15772 of which were unique ($R_{int}=0.0710$). The structure was refined on F^2 to 0.201, with $R(F)$ equal to 0.116 and a goodness of fit $S=2.39$.

Compound 11a·4C$_4$H$_8$O$_2$: $C_{42}H_{48}IN_4O_4$; crystals grew as long colorless needle and lathes on the wall of a test tube right after the column chromatography (silica gel, ethyl acetate/hexanes 1:9). The data crystal was cut from a large cluster of crystals and had approximate dimensions $0.48\times0.22\times0.11$ mm: monoclinic, space group $P2_1/n$, $a=20.1548(6)$, $b=6.5134(2)$, $c=28.2362(10)$ Å, $\alpha=\gamma=90°$, $\beta=91.508(2)°$, $V=3705.5(2)$ Å^3, $Z=4$, $\rho_{calcd}=1.206$ g cm^{-3}, $\mu=0.078$ mm^{-1}, $F(000)=1440$. A total of 476 frames of data were collected using ω-scans with a scan range of 0.8° and a counting time of 145 seconds per frame. A total of 11762 reflections were measured, 11762 of which were unique. The structure was refined on F^2 to 0.189, with $R(F)$ equal to 0.106 and a goodness of fit $S=1.94$.

CCDC-248670 (**9a**·2C$_3$H$_6$O), CCDC-248671 (**9a**·C$_{16}$H$_{36}$NNO$_3$), CCDC-248672 (**9a**·C$_{16}$H$_{36}$NCl), CCDC-248673 (**10a**·C$_{16}$H$_{36}$NNO$_3$·3CH$_2$Cl$_2$), CCDC-248674 (**10a**·C$_{16}$H$_{36}$NPF$_6$·3CH$_2$Cl$_2$), CCDC-248675 (**8a**), and CCDC-248676 (**11a**·4C$_4$H$_8$O$_2$) contain the supplementary crystollographic data for this paper. These data can be obtained free of charge from The Cambridge Crystallographic Data Centre via www.ccdc.cam.ac.uk/data_request/cif.

Acknowledgement

This work was supported by the National Institute of Health (Grant No. GM 58907 to J.L.S.) and Kraft Foods.

[1] P. A. Gale, J. L. Sessler, V. Kral, V. Lynch, *J. Am. Chem. Soc.* **1996**, *118*, 5140–5141.
[2] K. Kavallieratos, C. M. Bertao, R. H. Crabtree, *J. Org. Chem.* **1999**, *64*, 1675–1683.
[3] P. A. Gale, S. Camiolo, G. J. Tizzard, C. P. Chapman, M. E. Light, S. J. Coles, M. B. Hursthouse, *J. Org. Chem.* **2001**, *66*, 7849–7853.
[4] K. Sato, S. Arai, T. Yamagishi, *Tetrahedron Lett.* **1999**, *40*, 5219–5222.

[5] A. Szumna, J. Jurczak, *Eur. J. Org. Chem.* **2001**, 4031–4039.
[6] K. Choi, A. D. Hamilton, *Coord. Chem. Rev.* **2003**, *240*, 101–110.
[7] a) B. Turner, M. Botoshansky, Y. Eichen, *Angew. Chem.* **1998**, *110*, 2633–2637; *Angew. Chem. Int. Ed.* **1998**, *37*, 2475–2478; b) B. Turner, A. Shterenberg, M. Kapon, K. Suwinska, Y. Eichen, *Chem. Commun.* **2001**, 13–14; c) B. Turner, A. Shterenberg, M. Kapon, K. Suwinska, Y. Eichen, *Chem. Commun.* **2002**, 404–405; d) B. Turner, A. Shterenberg, M. Kapon, K. Suwinska, Y. Eichen, *Chem. Commun.* **2002**, 726–727.
[8] a) G. Cafeo, F. H. Kohnke, G. L. La Torre, A. J. P. White, D. J. Williams, *Angew. Chem.* **2000**, *112*, 1561–1563; *Angew. Chem. Int. Ed.* **2000**, *39*, 1496–1498; b) G. Cafeo, F. H. Kohnke, G. L. La Torre, A. J. P. White, D. J. Williams, *Chem. Commun.* **2000**, 1207–1208; c) G. Cafeo, F. H. Kohnke, G. L. La Torre, M. F. Parisi, R. P. Nascone, A. J. P. White, D. J. Williams, *Chem. Eur. J.* **2002**, *8*, 3148–3156; d) G. Cafeo, F. H. Kohnke, M. F. Parisi, R. P. Nascone, G. L. La Torre, D. J. Williams, *Org. Lett.* **2002**, *4*, 2695–2697.
[9] J. L. Sessler, P. Anzenbacher, Jr., J. A. Shriver, K. Jurisíková, H. Miyaji, V. Lynch, M. Marquez, *J. Am. Chem. Soc.* **2000**, *122*, 12061–12062.
[10] J. A. Shriver, Ph.D. Dissertation, The University of Texas at Austin (USA), **2002**.
[11] V. Král, P. A. Gale, P. Anzenbacher Jr., K. Jursíková, V. Lynch, J. L. Sessler, *Chem. Commun.* **1998**, 9–10.
[12] J. L. Sessler, W.-S. Cho, V. Lynch, V. Král, *Chem. Eur. J.* **2002**, *8*, 1134–1143.
[13] a)Y.-S. Jang, H.-J. Kim, P.-H. Lee, C.-H. Lee, *Tetrahedron Lett.* **2000**, *41*, 2919–2923; b) N. Arumugam, Y.-S. Jang, C.-H. Lee, *Org. Lett.* **2000**, *2*, 3115–3117; c) A. Nagarajan, J.-W. Ka, C.-H. Lee, *Tetrahedron* **2001**, *57*, 7323–7330.
[14] J. L. Sessler, D. An, W.-S. Cho, V. Lynch, *Angew. Chem.* **2003**, *115*, 2380–2383; *Angew. Chem. Int. Ed.* **2003**, *42*, 2278–2281.
[15] J. L. Sessler, D. An, W.-S. Cho, V. Lynch, *J. Am. Chem. Soc.* **2003**, *125*, 13646–13647.
[16] E.-C. Lee, Y.-K. Park, J.-H. Kim, H. Hwang, Y.-R. Kim, C.-H. Lee, *Tetrahedron Lett.* **2002**, *43*, 9493–9495.
[17] G. A. Sotzing, J. R. Reynolds, A. R. Katritzky, J. Soloducho, S. Belyakov, R. Musgrave, *Macromolecules* **1996**, *29*, 1679–1684.
[18] C. S. Wilcox in *Frontiers in Supramolecular Organic Chemistry and Photochemistry* (Eds.: H.-J. Schneider, H. Dürr), VCH, Weinheim, **1991**, pp. 123–143.
[19] K. A. Connors, *Binding Constants*, John Wiley, New York, **1987**.
[20] F. P. Schmidtchen, *Org. Lett.* **2002**, *4*, 431–434.
[21] Z. Otwinowski, W. Minor, *Methods Enzymol.* **1997**, *276*, 307–326.
[22] "SIR92: A program for crystal structure solution": A. Altomare, G. Cascarano, C. Giacovazzo, A. Guagliardi, *J. Appl. Crystallogr.* **1993**, *26*, 343–350.
[23] "SIR97: A program for crystal structure solution": A. Altomare, M. C. Burla, M. Camalli, G. L. Cascarano, C. Giacovazzo, A. Guagliardi, A. G. G. Moliterni, G. Polidori, R. Spagna, *J. Appl. Crystallogr.* **1999**, *32*, 115–119.
[24] G. M. Sheldrick, SHELXL97. Program for the Refinement of Crystal Structures, **1997**, University of Göttingen, Göttingen (Germany).
[25] *International Tables for X-ray Crystallography Vol. C* (Ed.: A. J. C. Wilson), Kluwer Academic Press, Boston, **1992**, Tables 4.2.6.8 and 6.1.1.4.

Received: August 31, 2004
Published online: December 29, 2004

